

Methods for Estimating Major Angles of Anisotropy in the Subsurface

November 4, 2025

Moses Obiri¹, Swasti Saxena², Deb Fagan¹,
Tollef Winslow³, **Jen (Huckett) Willis¹**

¹ Pacific Northwest National Laboratory (PNNL)

² Previously PNNL

³ Central Plateau Cleanup Company (CPCCo)

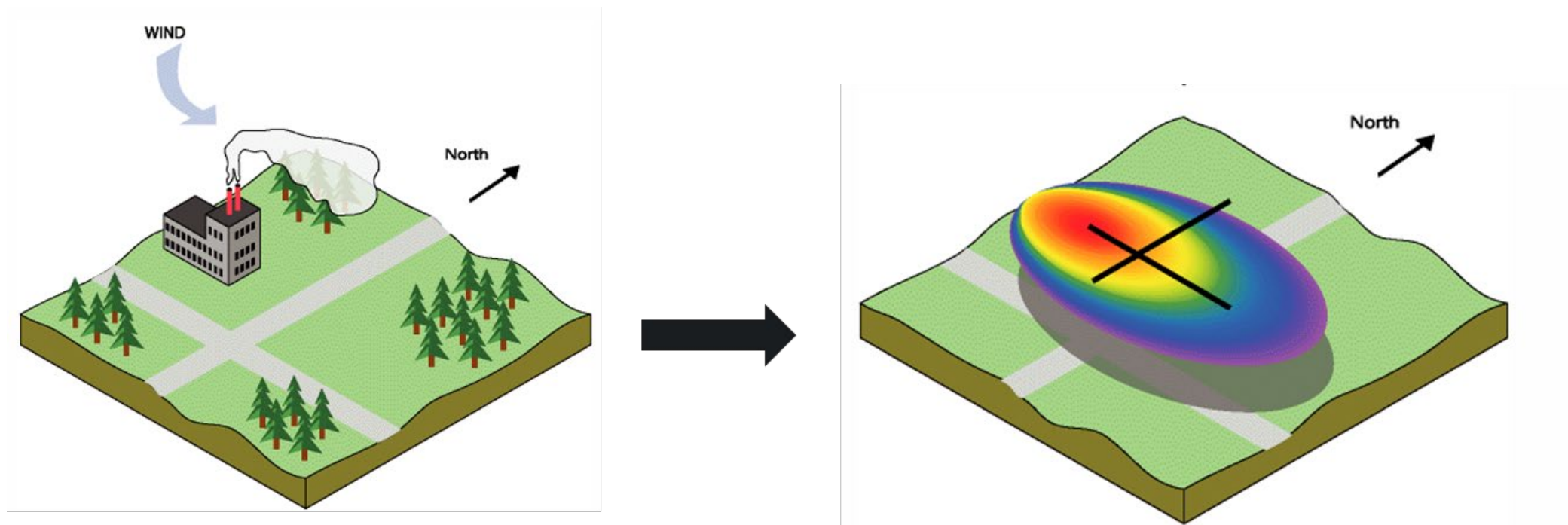
Overview

- Background
 - Anisotropy
 - Variogram analysis & automation
- Methodology
- Results/Hanford case study
- Implementation in Visual Sample Plan

Anisotropy

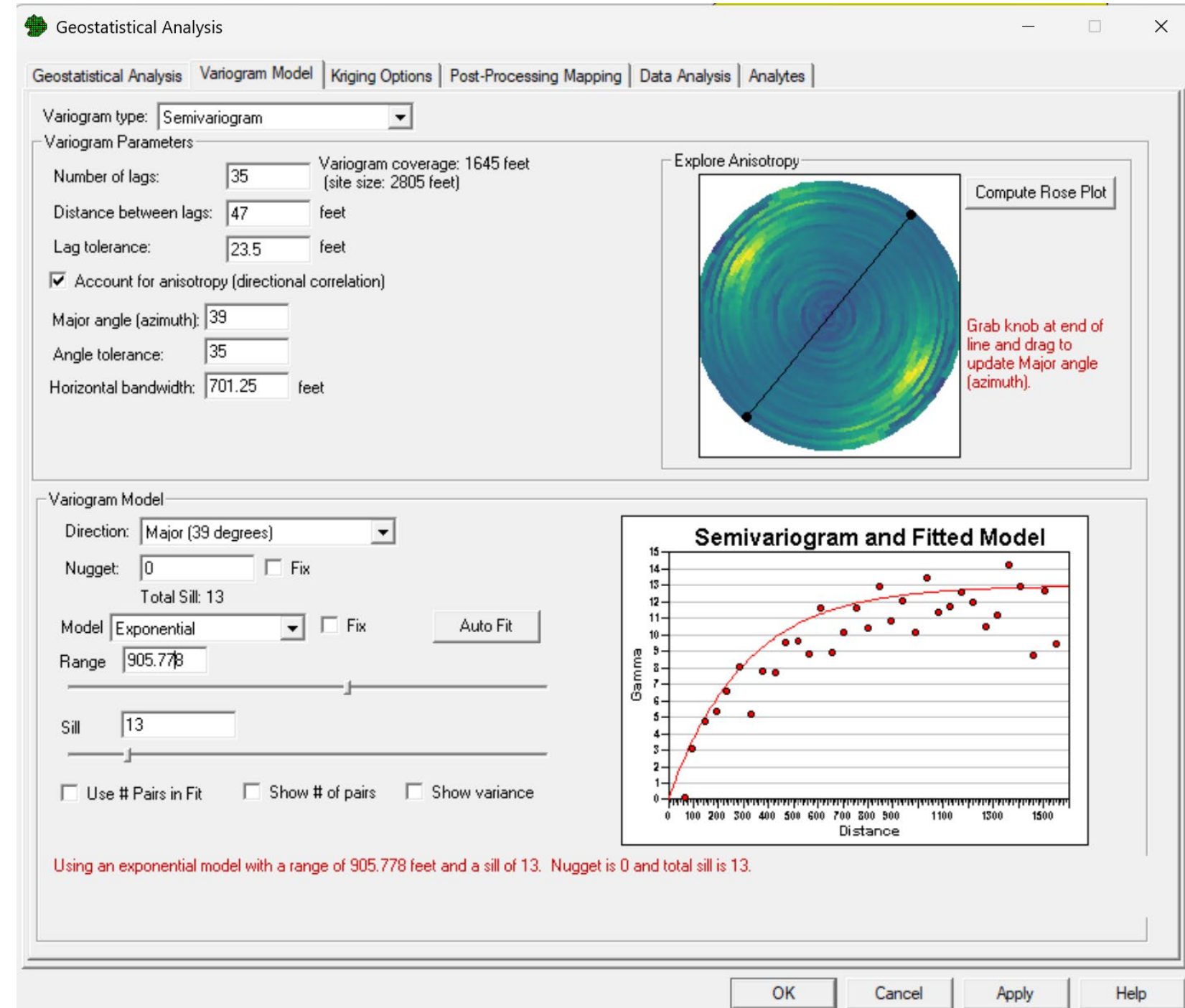
Occurs when spatial dependence is stronger in some directions than others

- Ex: due to wind directions – surface
- Ex: due to geomorphology – subsurface
- Some geospatial models incorporate anisotropy



Variogram Analysis

- Statistical representation of correlation as a function of distance.
 - **Isotropy:** variograms are the same in all directions.
 - **Anisotropy:** variograms differ depending on direction.
- Added Visual Sample Plan functionality that automates the variogram analysis for easier implementation.



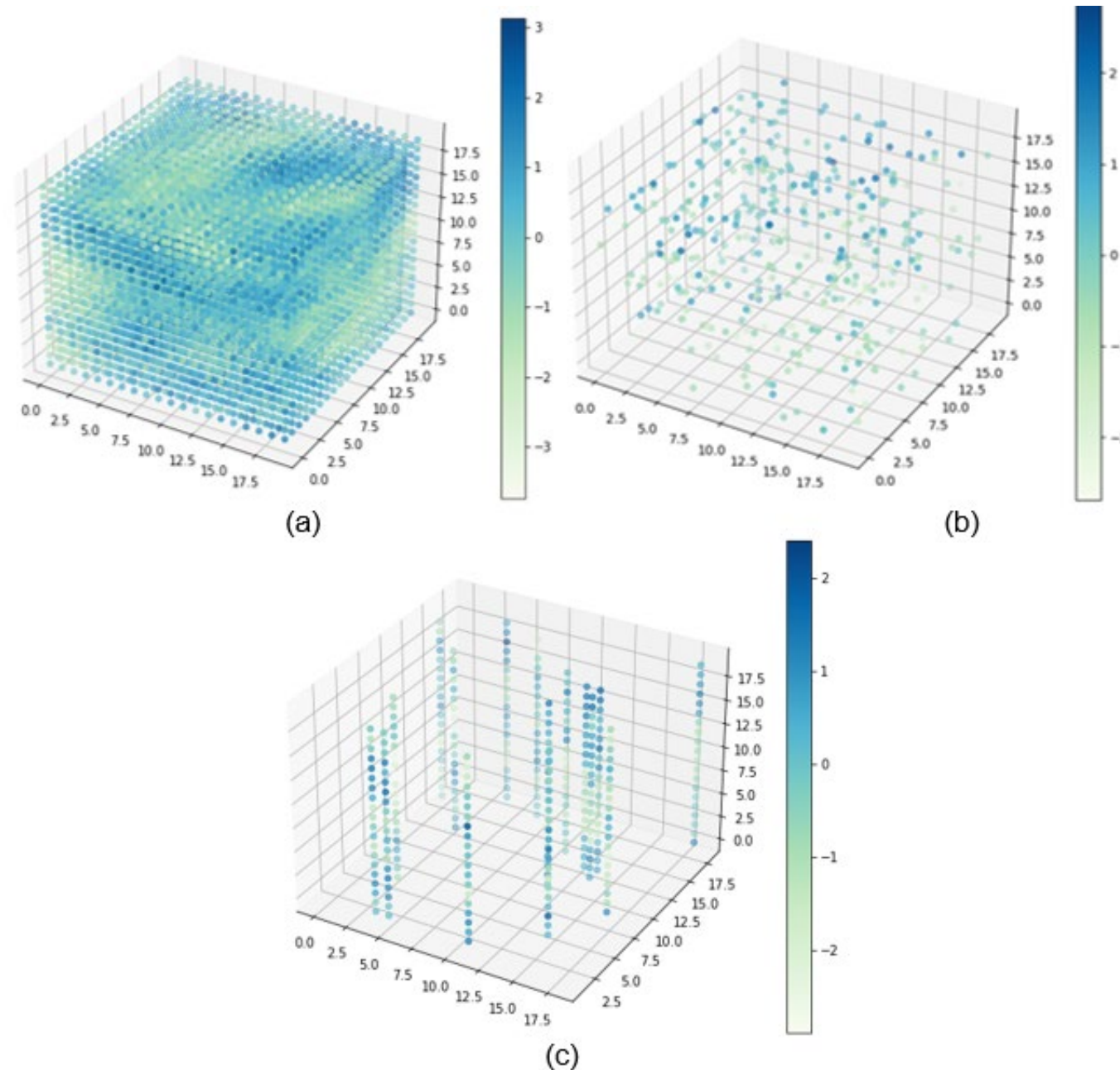
Approach

- Literature review identified few approaches to determining directions of anisotropy. PNNL identified MOI and CTI as most promising.
- Mass moment of inertia (MOI) (Hassanpour and Deutsch 2008)
 - Employs principles of MOI tensor, commonly used in classical mechanics to describe the rotation of a body, analyzing eigenvectors to estimate anisotropy directions (Goldstein et al. 2001).
 - Mathematical robustness and versatility in handling data from different dimensions and scales offer an approach to understanding spatial orientation.
- Covariance tensor identity (CTI) (Chorti and Hristopulos 2008)
 - Utilizes mathematics of covariance functions to determine anisotropy directions through solutions of nonlinear equations.
- Both methods previously developed in 2D frameworks. PNNL developed in 3D.
 - MOI: PNNL adapted the 2D MOI method to 3D by introducing a third dimension along the z-axis, resulting in a 3D tensor matrix.
 - CTI: PNNL developed a 3D approximation, where we applied the 2D CTI method to 2D slices of the 3D volume and calculated principal angle of anisotropy for each and then averaged the slice estimates.

Approach (cont.)

- PNNL adapted 2D MOI and CTI frameworks for 3D datasets for application to subsurface soil samples and surveys.
 - Demonstrated ability to systematically identify principal directions of anisotropy and evaluated performance for multiple types of subsurface datasets (randomly samples points, densely sampled boreholes/wells, sparsely sampled boreholes).
 - Initially developed and tested on simulated 2D and 3D datasets to provide a proof of concept.
 - Applied MOI and CTI to case study with data from Hanford Site.

Method Evaluation



Simulated Data

- (a) structured
- (b) unstructured
- (c) borehole data

Generated from 3D variogram models:

- Angles of anisotropy equal to $(\alpha, \beta, \gamma) = (45^\circ, 25^\circ, 10^\circ)$.
- Axes are in meters.

Dimension	Data Type and Number of Observations			
	Structured	Unstructured	Borehole	
			16 Boreholes	100 Boreholes
2D	400	400	n/a	n/a
3D	8000	400	320	2000

Results

Data Type	Sample Size (# Points)	True Angle of Anisotropy (°)	Estimated Angle of Anisotropy			
			MOI – 2D		CTI – 2D	
			Mean (°)	MAD (°)	Mean (°)	MAD (°)
Structured	400	30	33	15	33	6
Structured	400	45	44	8	45	5
Structured	400	60	60	17	58	6
Unstructured	400	30	33	11	43	22
Unstructured	400	45	33	13	11	36
Unstructured	400	60	57	10	57	11

Data Type	Sample Size	True Angles of Anisotropy (°)	Estimated Angles of Anisotropy			
			MOI – 3D		CTI – 3D	
			Mean (°)	MAD (°)	Mean (°)	MAD (°)
Structured	8000 points	45, 25, 10	40, 30, 19	7, 7, 11	62, 31, 15	24, 6, 7
		60, 30, 10	52, 20, 17	22, 11, 9	66, 34, 9	7, 6, 4
Unstructured	400 points	45, 25, 10	49, 17, 20	18, 11, 13	n/a	n/a
		60, 30, 10	68, 19, 18	27, 13, 12	n/a	n/a
Borehole	16 boreholes	45, 25, 10	59, 23, 32	20, 12, 25	n/a	n/a
	320 points	60, 30, 10	57, 15, 55	8, 17, 46	n/a	n/a
Borehole	100 boreholes	45, 25, 10	46, 17, 18	15, 10, 11	55, -2, 5	17, 27, 7
	2000 points	60, 30, 10	58, 16, 19	18, 15, 12	64, -1, 5	4, 31, 5

MAD = mean absolute deviation (uncertainty)

Assess Performance

Compare estimated to true angles of anisotropy.

- MOI estimates within 5-10° of the true angles of anisotropy with MAD $\pm 20^\circ$
- CTI estimates deviated from true angles of anisotropy more than MOI estimates, with similar MAD

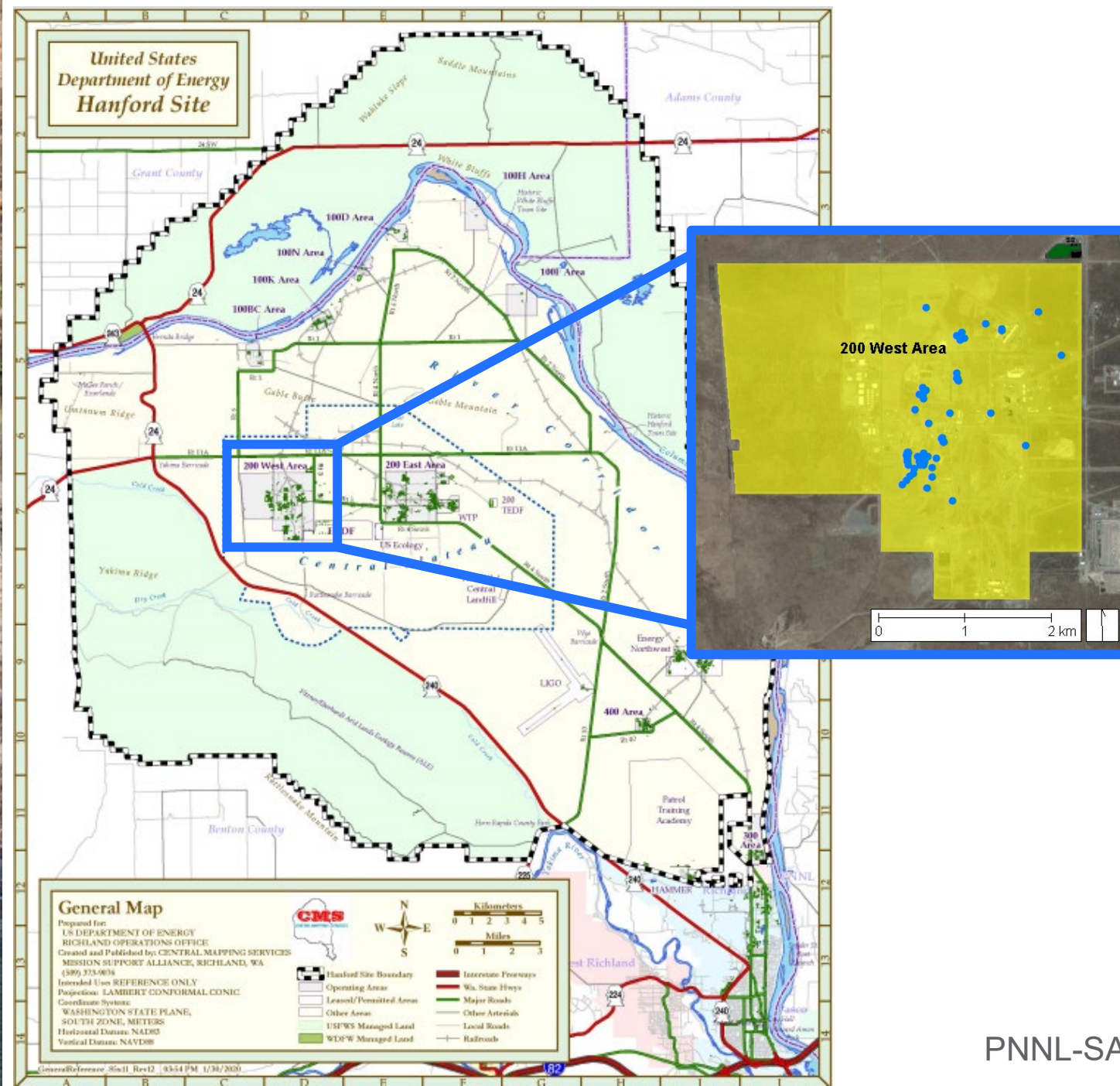
Hanford Case Study – Dataset

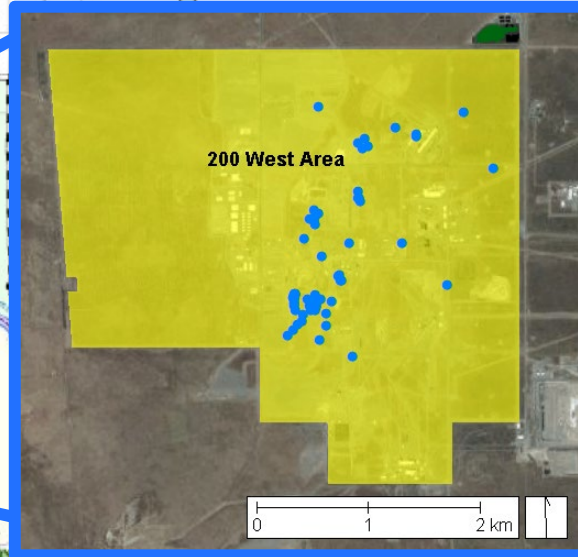
Geographic extent of 200 West Area is on the western side of the Hanford Site.

Curated borehole dataset, with input from Central Plateau Cleanup Company (CPCCo)—a prime contractor to the Department of Energy (DOE) environmental cleanup of legacy nuclear waste at the Hanford Site (CPCCo 2024) with expertise in Hanford Site data collection.

Dataset:

- Subset of all boreholes in the 200 West Area at locations shown with blue points
- Active in varying and timespans between 2002 and 2008
- Depths ranging 12–160 meters (40–525 ft)
- 8,800 datapoints total





Columbia River drainage paths in this area have changed from the inferred drainage path during the middle-to-late Ringold time (Reidel 2013) to current drainage path.

- Current Columbia River drainage path runs east and then north of where the 200 West Area is located, represented in blue and purple.
- Inferred Columbia River drainage path during the Ringold Formation runs south and west of where the 200 West Area is located, along where WA-243 is currently located (red line running from the bottom right at roughly a **135°** angle (from the southeast corner of the map) up to where it intersects WA-24 to the northwest of the 200 West Area).

Generalized Stratigraphy of 200 West Area

	Sedimentary Unit	Depositional Environment	Lithology	
HF1 HF2 HF3	Hanford formation – unit 1	Fluvial, mega floods	Gravel dominated quartz and basalt	<div>younger</div> <div>↑</div> <div>↓</div> <div>older</div>
	Hanford formation – unit 2	Fluvial, mega floods	Sand dominated quartz and basalt	
	Hanford formation – unit 3	Fluvial, mega floods	Gravel dominated quartz and basalt	
CCUc	Cold Creek unit	Lacustrine(?)	Silt and fine grained sand	
	Cold Creek unit – caliche	Lacustrine(?)	Silt and sand with a caliche overprint	
Ringold (Rwie)	Ringold Formation member of Taylor Flat	Fluvial	Interstratified deposits of fine-grained fluvial sand and silt.	
	Ringold Formation member of Wooded Island – unit E	Fluvial	Well-rounded fluvial gravel of mixed lithologies, in a sand and silt matrix; cementation varies.	
	Ringold Formation lower mud unit	Fluvial, overbank	Primarily lacustrine silt and clay, overlying a well-developed paleosol.	
	Ringold Formation member of Wooded Island – unit A	Fluvial	Generally a conglomerate with clasts of basalt and other lithologies in a silty sand matrix intercalated with beds of sand and silt; strongly cemented in places. A silt layer is present in some locations and acts as an aquitard for underlying sediments	

Applied MOI and CTI methods to the analysis dataset

- **3D volume:** single anisotropy estimate throughout
- **2D layered approach:** different anisotropy estimate by layer

Analysis Dataset

- Data
 - Spectral gamma gross counts
 - Potassium-40 (naturally occurring radionuclide present across the Hanford Site)
 - (x, y, z) coordinates
 - Sample dates and times
 - Geologic formation within each borehole and (x, y, z) coordinate
- 130 observations per borehole, on average
 - As few as 13 observations
 - Up to 486 observations

Borehole Identifier	x	y	Number of Observations
299-E25-184	136006.490	575323.615	62
299-E28-8	137074.300	573698.100	347
299-W10-21	137154.721	566583.991	259
299-W11-14	136913.962	567457.917	302
299-W11-43	136971.040	567269.740	486
299-W11-68	136782.453	566970.884	117
299-W11-69	136834.817	566929.293	121
299-W11-80	136873.284	566996.371	55
299-W11-81	136801.847	567024.200	56
299-W11-82	136407.518	566933.853	78
299-W11-86	136610.040	568143.530	179
299-W11-88	137113.090	567874.670	217
299-W14-1	136311.178	566953.318	253
299-W14-2	136340.409	566932.320	248
299-W14-3	136342.965	566940.409	250
299-W14-52	135936.513	566855.414	29
299-W14-71	135567.810	567733.430	321
299-W14-72	135941.280	567328.440	307
299-W15-10	135981.140	566448.629	254
299-W15-204	135827.610	566610.306	27
299-W15-209	136140.101	566545.409	55

... ..

Performance – 3D Volume Application

- Unlike simulated data, ground truth is unknown with real data
 - Use bootstrap re-sample to approximate sampling from boreholes at the site
 - Approximate the ‘truth’ using the whole dataset
 - Note that the Reidel 2013 hypothesis leads to **135°** angle

Radiological Measurement	Sample Size	Angles of Anisotropy (°) Ground Truth	Estimated Angles of Anisotropy (°) – Sampled Dataset			
			MOI – 3D		CTI – 3D	
			Mean (°)	MAD (°)	Mean (°)	MAD (°)
Potassium-40	70 boreholes 500 points	137, 83, 99	131, 83, 92	7, 1, 8	n/a	n/a
Gross Gamma	71 boreholes 500 points	125, 77, 96	125, 80, 89	2, 1, 7	n/a	n/a
Potassium-40	50 boreholes 500 points	137, 83, 99	141, 83, 96	14, 4, 16	n/a	n/a
Gross Gamma	50 boreholes 500 points	125, 77, 96	129, 75, 90	6, 4, 8	n/a	n/a

- **MOI accurately approximates ground truth**
 - Potassium-40: ground truth 137°, 83°, 99° ↔ MOI estimates 131°, 83°, 92° (MAD 7°, 1°, 8°)
 - Gross gamma: ground truth 125°, 77°, 96° ↔ MOI estimates 125°, 80°, 89° (MAD 2°, 1°, 7°)

Performance – 2D Layered Application

Radiological Measurement	Layer	Sample Size	Ground Truth Angle of Anisotropy		Estimated Angle of Anisotropy			
			MOI (°)	CTI (°)	MOI – 2D		CTI – 2D	
					Mean (°)	MAD (°)	Mean (°)	MAD (°)
Potassium-40	Hf1	66 boreholes 500 points	59	82	62	5	68	14
	Hf2	45 boreholes 500 points	40	76	40	1	66	11
	Hf3	22 boreholes 300 points	32	47	34	3	48	3
	CCU	32 boreholes 200 points	41	16	41	1	40	27
	Rwie	16 boreholes 300 points	113	74	121	9	40	34
Gross Gamma	Hf1	66 boreholes 500 points	58	73	58	1	67	7
	Hf2	45 boreholes 500 points	45	79	45	1	74	5
	Hf3	22 boreholes 300 points	38	49	39	1	49	3
	CCU	32 boreholes 200 points	44	71	44	1	71	1
	Rwie	16 boreholes 300 points	136	83	137	8	63	20

- Geologic processes reflected in different layers: angles of anisotropy differ by geologic layer → consider both 2D layers and 3D layers in future studies.
- Method results
 - MOI estimates closer to ground truth than CTI
 - MOI MAD values less than or equal to than CTI MAD values in all layers

Ringold Formation

- MOI estimated angles of anisotropy within geologic layer associated with Ringold Formation are consistent with inferred Columbia River drainage path (Reidel 2013)
 - Roughly 135° from the northwest corner of that map (north is 0° , east 90° , and northeast to southwest is 135°)
 - Validating accuracy of MOI estimate in that geologic layer
- Summary
 - 2D layered approach: MOI method consistently resulted in estimates similar to ground truth, whereas CTI method, while accurate in some layers, was inconsistent.
 - 3D volume approach: CTI method could not be applied due to limitations.

Findings & Conclusions

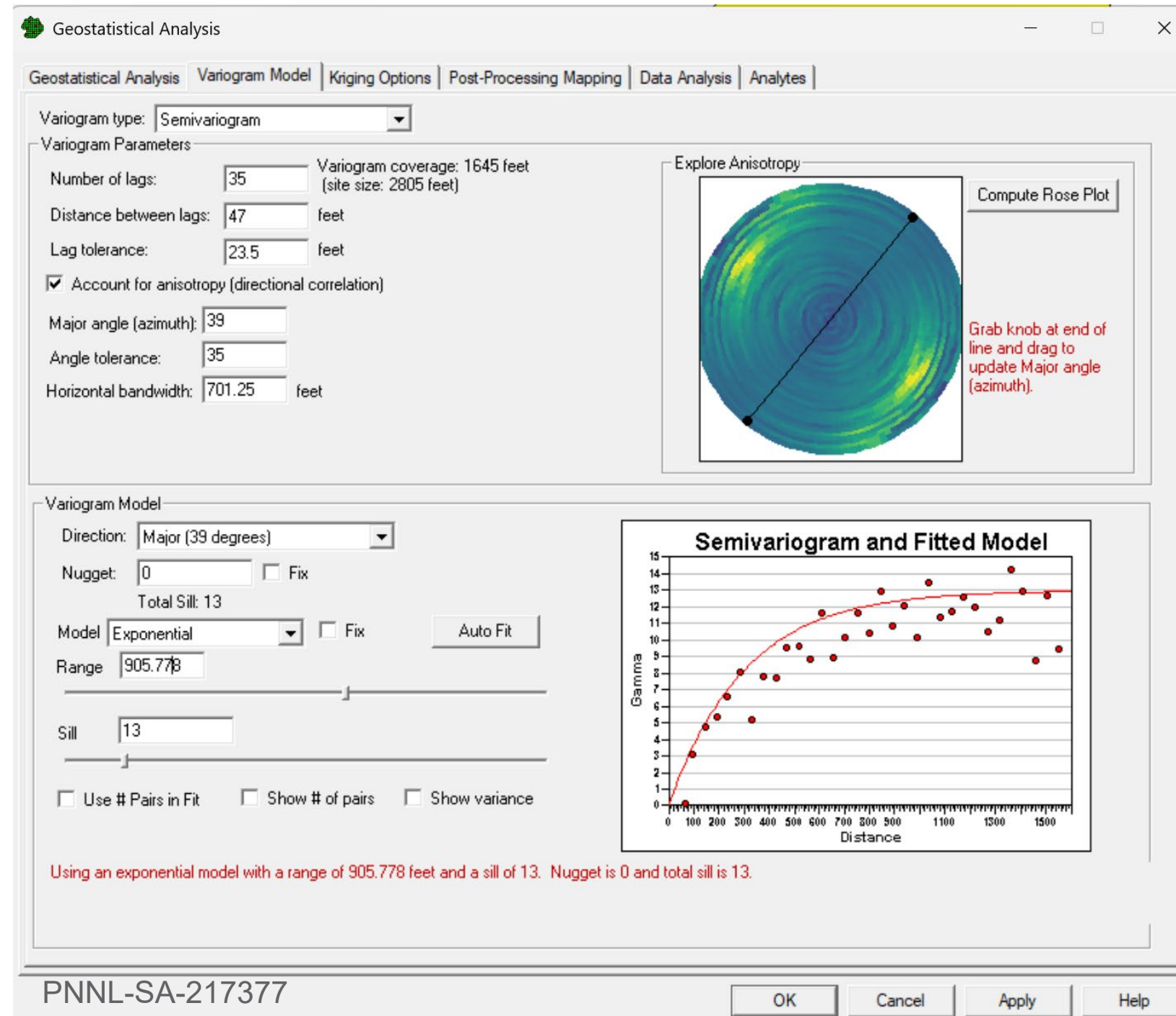
- Automating the selection of principal directions of anisotropy is particularly important for practitioners considering surveys for subsurface decommissioning and new borehole and well placement.
 - Both 2D layered approach and 3D volume approach should be examined.
 - Especially when geologic/other potential subsurface conditions could affect layers.
- PNNL assessed MOI and CTI as potential methods that could be implemented in VSP to assist with determining the principal directions of anisotropy.
 - Both methods performed well in structured datasets and produced less accurate estimates in unstructured datasets (simulations).
 - MOI produced more accurate and precise results than the CTI, when compared to ground truth, in simulated and real borehole data.
 - MOI method estimated primary and secondary angles of anisotropy within default angular tolerance (22.5°) applied in practice by most geostatistical software (Müller et al. 2022).
- **MOI method is more reliable and versatile than CTI.**

PNNL implementing MOI in VSP.

- Surface (2D) functionality is available in current VSP (Version 7.24, released 7/28/2025).
- Subsurface (3D) functionality is under development.

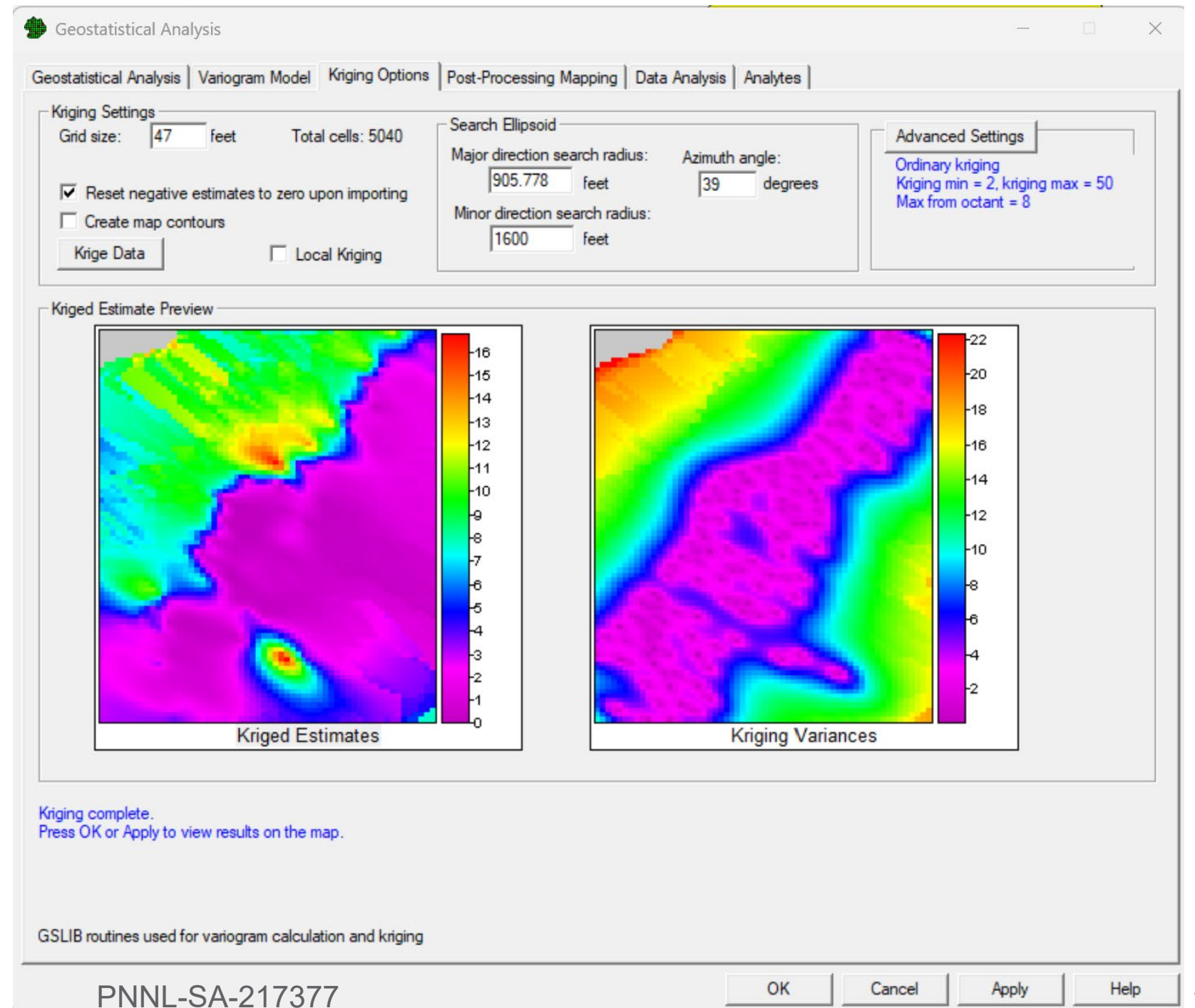
Visual Sample Plan (VSP)

www.pnnl.gov/projects/visual-sample-plan



Functionality

- VSP calculates variograms in all directions to produce a rose plot diagram for visualization of anisotropy
- 2D MOI method automatically determines the principal angle of anisotropy, with option for the user to adjust based on visual inspection of the rose plot diagram
- VSP automatically calculates and fits variogram models for the major and minor directions of anisotropy, and allows the user to adjust the fit parameters for a better fit



Thank you

Jen (Huckett) Willis: jen.willis@pnnl.gov
Debbie Fagan: deborah.fagan@pnnl.gov